Comparison between Fatigue Life Values Calculated Using Standardised and Measured Stress Spectra of a Naval High speed Light Craft

Teresa Magoga[1)2)], Seref Aksu[1)], Stuart Cannon[1)], Roberto Ojeda[2)], and Giles Thomas[3)]

[1)] Defence Science and Technology Group, Australia
[2)] Australian Maritime College, University of Tasmania, Australia
[3)] University College London, United Kingdom

Abstract

This paper presents a comparative study between assumed stress spectra and stress spectra derived from hull monitoring system data, with respect to the fatigue life at three different welded joints of a naval high speed light craft. The Palmgren-Miner rule, combined with Eurocode 9 construction details and fatigue resistance data, is applied to the stress spectra to calculate the fatigue life. This work has been motivated by the need to improve life-of-type evaluations of high speed naval vessels with semi-planing hullforms, which are required to perform demanding operations. It is shown that stress spectra derived from full-scale measurements are best modelled by Gaussian functions. Use of the largest stress cycle corresponding to design sagging and hogging load cases leads to conservative fatigue life estimates in comparison to analysis based on the derived spectra and fleet maintenance data, even when a 10^{-8} probability of sustaining the design loads is considered. The use of standardised stress spectra in fatigue analysis of naval high speed light craft offers benefits though requires further consideration of the characteristic fatigue loads and wave environments.

Keywords

Aluminium welded joints, fatigue, high speed light craft, stress spectrum

Introduction

Fatigue loading on ships is mainly due to combined global wave and slamming induced stresses (Fricke and Paetzold, 2010). Slamming occurs when the bow of a ship emerges from one wave crest and then re-enters with significant impact into the next wave. This can impart significant local impact loads and cause hull girder whipping; high frequency hull vibrations at a frequency near that of the hull's natural frequency. The whipping responses are superimposed on the low frequency wave load responses and significantly increase the number and magnitude of fatigue loading cycles (Phelps and Morris, 2013). For high speed light craft (HSLC) slam induced stresses can be relatively large due to the light displacement, shallow draft, and rela-tively high speed operations in varying sea environments (Magoga *et al.*, 2014). This is particularly the case for small naval vessels required to maintain a high operational tempo (Sheinberg *et al.*, 2011; Tuitman *et al.*, 2013).

With increasing use of semi-planing and planing hullforms and lightweight materials such as marine-grade aluminium, in addition to examples of fatigue failures in such craft, the need to develop rigorous lifetime load spectra has been recognised (Collette and Incecik, 2006; Engle *et al.*, 1997; Kramer *et al.*, 2006; Magoga *et al.*, 2015). Options to establish a lifetime fatigue load spectrum, required in fatigue life evaluation, include spectral analysis, time-domain analysis, and simplified analysis. Spectral analysis considers the operational conditions of a ship by dividing different operational modes by speed, heading, and significant wave height for a specific wave scatter diagram. Typically, this method assumes linear load effects and stress responses, and is performed in the frequency domain. However, its utilisation to accurately estimate load distributions and actual stress ranges of HSLC is restricted due to the difficulty in predicting the highly nonlinear relationship between applied loading and fatigue life (Collette and Incecik, 2006; Det Norske Veritas, 2011). In comparison, there are time-domain seakeeping codes available to calculate nonlinear loads to be transferred to structural models. However, coupled hydrodynamic-structural analysis is very time intensive, has tended to be limited to assessment of details, and requires validation via full-scale trials data (Sheinberg *et al.*, 2011; Tuitman *et al.*, 2013). In view of the above issues, it is suggested that practical procedures to generate standardised load histories for implementation in simplified fatigue life prediction of HSLC may be of benefit (Kramer *et al.*, 2000).

Simplified fatigue analysis assumes a stress history or spectrum at the detail, characterised by the shape, mean and maximum of the stress cycles. An appropriate probability level is allocated to a reference stress. Stresses are generally based on rule loads and may be calculated by an analytical approach or the Finite Element Method. As summarised by Horn *et al.* (2009), many classifica-

tion societies assume that the long term distributions of stress ranges at local details are described by the Weibull distribution. This interpretation differs from a study of strain measurements of commercial ships which, as summarised by Fricke and von Lilienfeld-Toal (2008), demonstrated that the long-term distribution of cyclic stresses induced by wave loads is largely linear. This latter approach is provided in Germanischer Lloyd's (GL) Rules for Classification and Construction – Seagoing Ships (2013).

Nonetheless, from a review of the literature and classification rules by the authors, there appears to be little information on the applicability of standardised stress spectra for HSLC. Design guidance for fatigue life estimation of HSLC receives less support than for steel ships (Soliman *et al.*, 2015). As such, there is a level of uncertainty associated with use of simplified fatigue analysis for HSLC, especially for naval vessels operating in demanding environments.

This paper presents a comparative study between assumed stress spectra and derived stress spectra from strain measurements, with respect to the fatigue life at three structural details of naval aluminium HSLC. The study platform is an aluminium patrol boat, for which the results of finite element analysis and hull monitoring system data are available. Using this information, the accuracy of Linear, Gaussian and Weibull modelling of the derived stress spectra is investigated in two ways; firstly via goodness of fit, and secondly by comparing the fatigue life at the three details based on the derived and modelled spectra. The fatigue life is estimated using the Palmgren-Miner rule applied to fatigue resistance data for welded aluminium structures. This is followed by an examination of the sensitivity of fatigue analysis to standardised stress spectra, characterised by the maximum and number of stress cycles. Finally, recommendations for further work are proposed. The results of this study enable the informed selection of the service life stress spectrum for use in life-of-type evaluation of naval HSLC with demanding operational requirements.

Analysis

Study Platform

The study platform is the 56 m Royal Australian Navy Armidale Class Patrol Boat (ACPB). The ACPBs feature a semi-planing hullform, and were constructed from marine-grade aluminium alloys. The vessels were designed and built by Austal Ships and classed by Det Norske Veritas (DNV) to be compliant with High Speed, Light Craft and Naval Surface Craft rules (Det Norske Veritas, 2011). The design life of the ACPBs is 20 years.

Finite Element Analysis

Finite Element Analysis (FEA) is utilised for the fatigue life evaluation. A global model of the ACPB structure has been developed, and validated, in the commercial FEA package MAESTRO 10.0.1 (2013). The model is shown in Fig. 1.
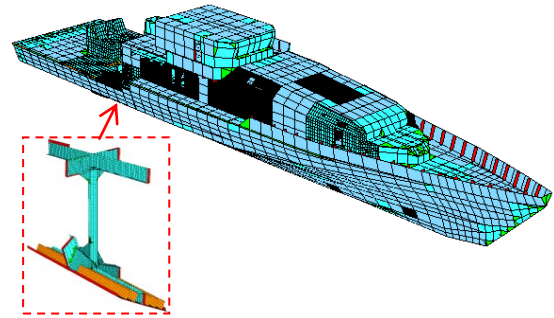

Fig. 1: Finite element model of ACPB with example embedded fine mesh

The overall stiffness of the structure is represented in the model. The mesh is relatively coarse to compute the global stress distribution of primary members of the hull, though several areas of the model have undergone mesh refinement (embedded fine mesh models) to allow geometric stress concentrations to be resolved. These include nominal stresses, stresses due to structural discontinuities, and attachments. In general, the model has shell elements for plating and areas of mesh refinement, and beam elements for stiffeners and girders.

Analysis of Hull Monitoring System Data

During the build of the last ACPB, HMAS GLENELG, the Defence Science and Technology Group collaborated with Austal Ships to commission a Hull Monitoring System (HMS). The aims of the project were to develop a structural fleet management capability, and to demonstrate the application of a versatile network using specialised sensors on a naval platform (Gardiner *et al.*, 2008). The HMS operated from May 2009 to February 2014.

The HMS was comprised of accelerometers, strain gauges, torsionmeters to measure shaft power, a six degree of freedom rigid body motion reference unit, and a Global Positioning System (GPS). The sensors were programmed to continuously collect and return data to a computer for storage. Most of the strain gauge signals were sampled at 50 Hz.

In this paper data from three strain gauges are considered. The locations of these gauges are displayed in Fig. 2. Strain gauges A, B and C were installed in 2012, in order to better understand the stresses induced in a pillar and the surrounding structure in the engine room:

- Strain gauge A was situated below the weld toe of the forward bracket of the pillar.

- Strain gauge B was installed 0.55 m aft of the pillar, on the underside of the main deck plating, approximately 0.45 m inboard from the deck edge.

- Strain gauge C was attached to the centre of the flange of a longitudinal beam underside of the main deck, approximately 0.4 m aft of the pillar.

Data processing routines were developed in MATLAB® R2014a to convert and filter the raw strain data to stress. Due to the susceptibility of strain measurements to electrical interference from surrounding electrical equipment and to offset changes in the signal amplification circuitry, spikes or single data measurements signifi-

cantly different to the preceding and subsequent measurements are present in the raw data. As such, the data processing routines include signal conditioning to remove spikes and to account for large offsets. High frequency noise was attenuated by applying a low-pass Chebyshev filter at 7.5 Hz, greater than the three-node bending vibration frequency of 5 Hz (Magoga *et al.*, 2014), to the signals.
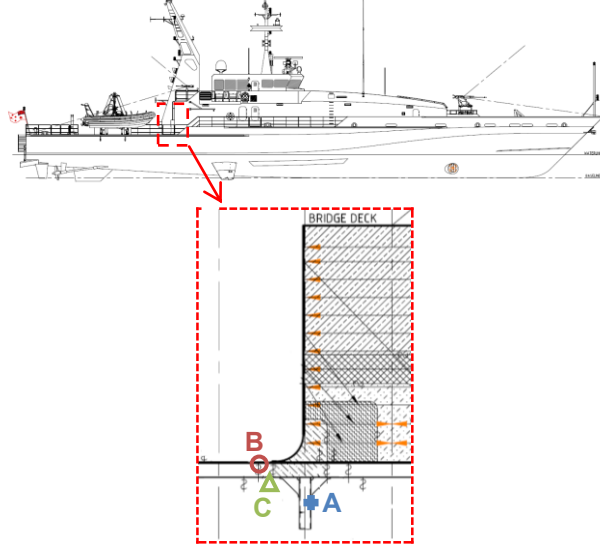

Fig. 2:   **Strain gauge locations, at pillar centreline**

A ship-based instrument to measure the encountered wave environment could not be installed onboard HMAS GLENELG. However, significant wave height statistics over a 2.5 year period of the ACPBs' primary operational area, the North-West of Australia, indicate that the vessels may have been operated 86% of the time in seas up to the top of Sea State 4, 13% in Sea State 5, and 1% in Sea State 6 (Aksu *et al.*, 2015). For perspective, the ACPBs were designed to maintain operations in Sea State 5 and to survive cyclonic conditions up to Sea State 9 (2006).

The collection of data was not continuous due to system defects, and maintenance of the vessel requiring power to the HMS to be switched off. As such, the total measurement duration between August 2012 and February 2014 was approximately 4500 hours. HMAS GLENELG was at sea 75% of this time. The corresponding speed profile is presented in Fig. 3.
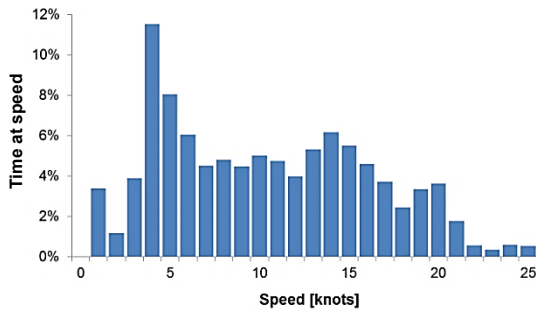

Fig. 3:   **HMAS GLENELG's speed profile between August 2012 and February 2014**

Stress Spectra Derivation

The stress spectra for strain gauges A, B, and C, generated using rainflow counting (Matsuishi and Endo, 1968), are shown in Fig. 4. The measured stress direction for strain gauge A is vertical, and for strain gauges B and C is longitudinal. To enable comparison of the different stress spectra, the stress shown on the y-axis is normalised by the allowable stress σ_{allow} of the ACPB calculated using DNV rules (2011).
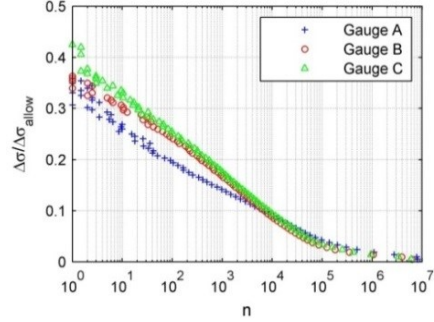

Fig. 4:   **Stress spectra derived from strain gauge data, normalised by $\Delta_{\sigma_{allow}}$ of ACPB**

The maximum measured stress cycle at the strain gauge locations considered ranges between approximately 35% and 45% of σ_{allow} of the ACPB. This outcome is not unexpected, as the design condition should be more severe than the worst intended condition by a suitable margin (Mansour and Liu, 2008).

To investigate the accuracy of form fitting of each of the derived stress spectra, the spectra have been modelled using the Linear (Eq. 1), Gaussian (Eq. 2), and Weibull (Eq. 3) functions:

$$\Delta\sigma = a\log(n) + b \tag{1}$$

$$\Delta\sigma = a_1 e^{\left(-\left(\frac{\log(n)-b_1}{c_1}\right)^2\right)} \tag{2}$$

$$\Delta\sigma = a_2\lambda\chi\log(n)^{(\chi-1)} e^{(-\lambda\log(n))} \tag{3}$$

Where a and b are the coefficients of the Linear function, and a_1, b_1, and c_1 are the coefficients of the Gaussian function. The scale and shape parameters of the Weibull function are denoted by λ and χ respectively, and a_2 is a scale parameter independent of the exponent term. The form fitting is conducted by the method of least squares.

The form fitting is based on stress cycles normalised by the design stress range $\Delta\sigma_{design}$ which differs at each strain gauge location. The values of $\Delta\sigma_{design}$ are computed using FEA under the design hogging and sagging load cases.

The coefficients of the Linear, Gaussian and Weibull models of the stress spectra for each strain gauge individually and combined (aggregate) are given in Table 1. The intention of the aggregate coefficients is to provide rationalised stress spectra for structural details indicative of those in the vicinity of the strain gauge locations (that is, pillars and supporting structural items). The goodness of fit R^2 values, shown in Table 2, indicate that the stress spectra are best approximated by a Gaussian model. Although the R^2 values of the Weibull models are also relatively high, there is unphysical decay at small values of n.

Table 1: Individual and aggregate coefficients of Linear, Gaussian and Weibull models, for each derived stress spectrum, based on stress cycles normalised by $\Delta\sigma_{design}$

Function		Strain Gauge			Aggregate
		A	B	C	
Linear	a	-0.180	-0.174	-0.186	-0.180
	b	1.000	1.000	1.000	1.000
Gaussian	a_1	1.000	1.000	1.000	1.000
	b_1	-1.338	-0.700	-0.898	-0.979
	c_1	4.401	4.138	4.055	4.198
Weibull	a_2	0.366	0.360	0.367	0.364
	λ	1.072	1.234	1.148	1.152
	χ	2.800	3.011	2.791	2.867

Table 2: Comparison between R^2 values of Linear, Gaussian and Weibull fits of stress spectra at each strain gauge location, using individual and aggregate coefficients

Function	R^2	Strain Gauge		
		A	B	C
Linear	Original	0.915	0.967	0.959
	Aggregate	0.915	0.964	0.956
	Difference	0%	0.30%	0.31%
Gaussian	Original	0.986	0.984	0.991
	Aggregate	0.979	0.956	0.990
	Difference	0.70%	2.8%	0.10%
Weibull	Original	0.983	0.977	0.975
	Aggregate	0.961	0.942	0.973
	Difference	2.2%	3.7%	0.23%

The derived and assumed stress spectra, using the aggregate coefficients, for strain gauges A, B, and C are compared in Fig. 5, 6 and 7 respectively. As the stress spectra follow distributions, and there is adequate coverage of the speed range, the measurement period is considered to provide an adequate long-term distribution of stress cycles.
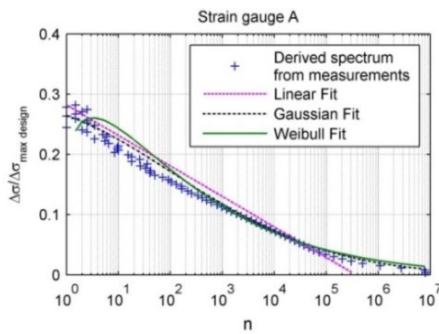

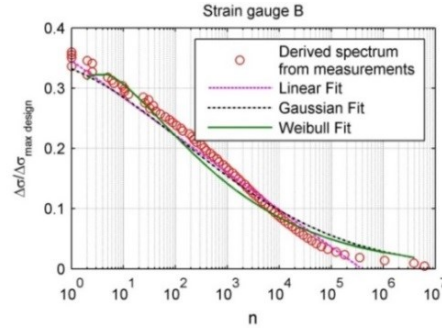Fig. 5: Comparison of strain gauge A derived and assumed stress spectra

Fig. 6: Comparison of strain gauge B derived and assumed stress spectra
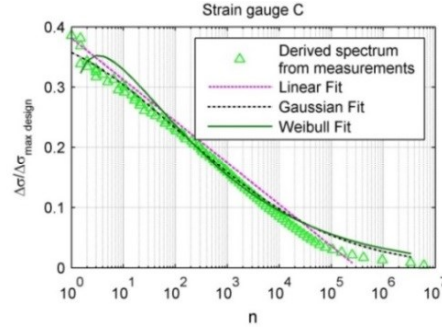

Fig. 7: Comparison of strain gauge C derived and assumed stress spectra

Fatigue Damage Estimation

The Palmgren-Miner rule (Miner, 1945) is used to calculate the fatigue damage. The damage D caused by all cycles is calculated using Equation 4:

$$D = \sum_{i=1}^{k} \frac{n_i}{N_i} = \frac{1}{\bar{a}} \sum_{i=1}^{k} n_i \left(\Delta\sigma_i\right)^m \tag{4}$$

Where k is the number of stress ranges, $\bar{a}$ and m are $\Delta\sigma$-N curve parameters, and n_i and N_i are the number of actual cycles experienced and cycles to failure for the ith stress range increment, respectively.

The fatigue life (FL) of a structural detail is the ratio of the service life, in years, to the fatigue damage. If the fatigue damage is less than unity, the structure has a fatigue life longer than the service or design life.
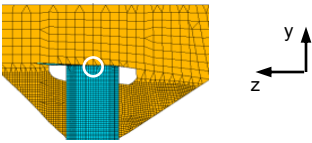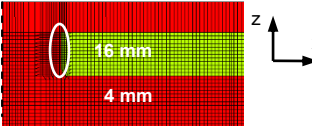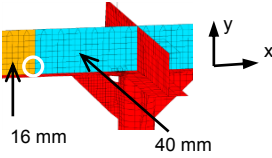
To assess the fatigue life of a detail, the structural (or geometric) stress approach is used. This approach entails determining the geometric stresses of a reference detail (strain gauge location) and the detail of interest using FEA, and then obtaining the ratio between the two values. In the calculation of the stress ratios between the locations of interest and the respective reference strain gauges, the maximum and minimum directional stresses under the design sagging and hogging load cases are taken. The ratio is then applied to the stress spectra. The construction detail with known fatigue resistance should be as similar as possible to the detail being assessed with respect to geometry and loads (Technical Committee CEN/TC 250, 1999).

Three structural details of interest are analysed. These details and the reference strain gauges are given in Table 3. Fatigue resistance data from Eurocode 9 (Technical Committee CEN/TC 250, 1999) is utilised, and the selected detail categories and corresponding constant

amplitude fatigue limits $\Delta\sigma_L$ are also given in Table 3. The reference gauges are selected due to the close vicinity to the location of interest, consistency of the dominant load direction, and similarity of construction detail.

When using the structural stress approach, it is essential that the stress type and value effectively describe the structural behaviour of the component (Horn *et al.*, 2009). To conduct the fatigue analysis at structural details with discontinuities and complex stress distributions, care was taken to refine the model in order to resolve the stress field at potential crack initiation sites using the recommendations given by DNV (Det Norske Veritas, 2010), Maddox (2003), and in Eurocode 9 (Technical Committee CEN/TC 250, 1999).

Table 3:   Analysed details of interest

Location	Construction Detail
ID-1 (Reference strain gauge is strain gauge A, stress ratio = 2.64) Top of pillar, forward side 	9.1 $\Delta\sigma_L$ = 12.3 MPa Double fillet weld
ID-2 (Reference gauge is strain gauge B, stress ratio = 2.38) Vicinity of weld seam between insert and main deck plating 	7.2.3 $\Delta\sigma_L$ = 18.1 MPa Butt weld of an open shape, welded from both sides
ID-3 (Reference gauge is strain gauge C, stress ratio = 1.78) Web of longitudinal under main deck, adjacent to fillet weld to flange and butt weld to plating of different thickness 	11.3 $\Delta\sigma_L$ = 18.1 MPa Cross-welded built-up beam, using double sided full penetration welding

Sensitivity of Fatigue Life to Fitted Spectra

The spectra are based on stress cycles incurred over approximately 4500 hours. Thus, to calculate the fatigue life considering a service period of 20 years, the spectra are linearly extrapolated.

Table 4 provides the estimated fatigue life for details ID-1, ID-2, and ID-3 based on the derived, Linear, Gaussian and Weibull spectra. The fatigue life values based on the reference derived spectra are consistent with fleet maintenance data, and are used to normalise the fatigue life values based on the assumed spectra for each detail.

Table 4:   Fatigue life estimates using different stress spectrum models at details of interest, normalised by fatigue life values based on derived spectra

ID	Derived spectrum	Linear spectrum	Gaussian spectrum	Weibull spectrum
1	1.00	0.738	0.980	0.767
2	1.00	0.841	1.35	1.31
3	1.00	0.565	0.907	0.872

The results given in Table 4 indicate that when a Linear model is used to represent the stress spectra at the strain gauge locations, the corresponding fatigue life estimates are smaller than those based on the derived spectra by an average of 29%. The Weibull model performs better, as the average difference (absolute) between the fatigue life estimates is 22%. In comparison, the fatigue life estimates based on the Gaussian spectra are most comparable with those based on the derived spectra, as the average difference is 15% (absolute).

Sensitivity of Fatigue Life Estimation to Standardised Lifetime Spectra

As discussed in the introduction, in the absence of detailed long term distributions of stresses, an approach provided by GL's Rules for Classification and Construction – Seagoing Ships (2013) is to use standardised linear spectra as shown in Fig. 8. Convex spectra can also be used with agreement from the society. The stresses range between the maximum and minimum stresses resulting from the maximum and minimum relevant seaway induced load effects, that is $\Delta\sigma_{design}$.
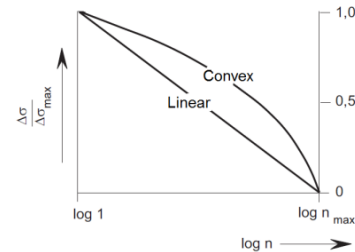

Fig. 8:   Standard stress range spectra given by GL (2013)

To test the applicability of standardised lifetime spectra to the three details of interest, the linear and convex spectra with the maximum stress range considered to occur once (n_{min} equals 10^0) are used to estimate the fatigue life. It is generally assumed that the number of stress cycles that a ship structure will experience over its life is 10^8 stress cycles. As such, when generating the spectra the sum of the number of cycles considered is 10^8 occurring during the design life of 20 years. In addition the number of stress increments needs to be sufficiently large to ensure reasonable numerical accuracy and should not be less than 20 (Det Norske Veritas, 2010). In this analysis 60 increments are used.

Table 5 shows the fatigue life based on the standardised linear and convex spectra with n_{min} equal to 10^0 at each detail of interest, as a percentage of the fatigue life based on the derived spectra. For details ID-1, ID-2, and ID-3 the fatigue life estimates based on the standardised linear spectra are 4.1%, 2.8% and 4.9% of the fatigue

life based on the derived spectra, respectively. Using the standardised convex spectra the fatigue life estimates at all three details are less than 1% of those based on the derived spectra. The standardised convex spectrum features more significant stress cycles over a greater range of n. Thus, its use leads to more conservative fatigue life estimates than the standardised linear spectra. However, for n_{min} equal to 10^0 both standardised spectra result in considerably smaller fatigue life values than those predicted using the measured strain data.

Table 5: Percentage fatigue life based on standardised linear and convex spectra, relative to that based on derived spectra, for each detail of interest

Detail	Spectrum	n_{min}		
		10^0	10^{-2}	10^{-4}
ID-1	Linear	4.1%	9%	18%
	Convex	0.59%	1.2%	2.2%
ID-2	Linear	2.8%	6.4%	13%
	Convex	0.41%	0.8%	1.5%
ID-3	Linear	4.9%	11%	23%
	Convex	0.69%	1.4%	2.6%

When n_{min} is equal to 10^0, it is accepted that the structure will sustain the design loads once in its lifetime. Thus, application of standardised spectra with n_{min} equal to 10^0 is unrealistic. Therefore, standardised spectra with probabilities of 10^{-2} and 10^{-4} of the structure sustaining the design loads are additionally considered as plotted in Fig. 9.
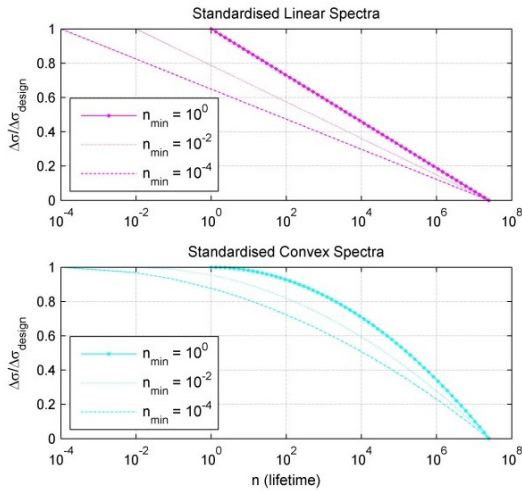

Fig. 9: Standardised Linear and Convex stress range spectra, with n_{min} equal to 10^0, 10^{-2}, and 10^{-4}

To check the validity of defining the standardised spectra by smaller probabilities of the structure sustaining the design loads, the subsequent relationships between increments of n_i/N_i ($D_i = n_i/N_i$) and $\Delta\sigma/\Delta\sigma_{design}$ are compared to those based on the derived spectra. For example, for detail ID-1, Fig. 10a, b, c, and d display the relationship between n_i/N_i and $\Delta\sigma/\Delta\sigma_{design}$ based on the derived spectrum of the reference strain gauge, the linear spectrum with n_{min} equal to 10^0, the linear spectrum with n_{min} equal to 10^{-2}, and the linear spectrum with n_{min} equal to 10^{-4}, respectively. Note that the y-axis scale of the derived spectrum plot (a) is smaller than the y-axis

scale of the linear spectra plots (b, c and d) because the measurement period, and hence number of cycles, was considerably less than assumed during the design life used to generate the linear spectra.
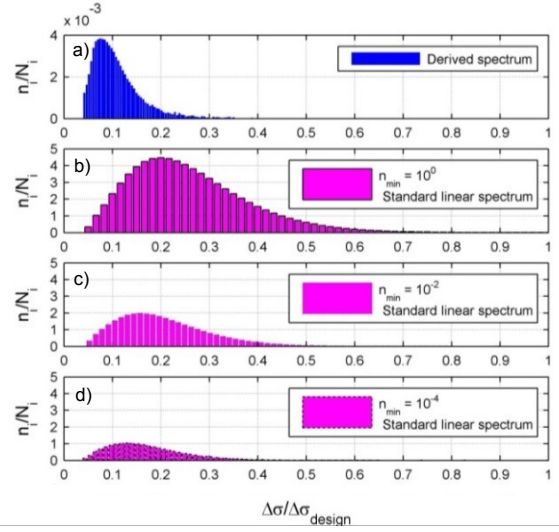

Fig. 10: $\Delta\sigma/\Delta\sigma_{design}$ versus n_i/N_i based on a) derived stress spectrum, and standardised linear spectra with n_{min} equal to b) 10^0, c) 10^{-2}, and d) 10^{-4}, at detail ID-1 (note y-axis scale of plot a) differs from b), c) and d))

Fig. 10a reveals that at detail ID-1 the combination of the fatigue resistance data for Eurocode 9 construction detail 9.1 (see Table 3) and the distribution of the stress cycles measured at reference strain gauge A results in the largest contribution to fatigue damage (n_i/N_i) occurring at approximately 7% of $\Delta\sigma_{design}$. For the linear spectra with n_{min} equal to 10^0, 10^{-2}, and 10^{-4} the fatigue damage peaks occur at 20%, 16%, and 13%, respectively, of $\Delta\sigma_{design}$ (see Fig. 10b, c and d). For all spectra n_i/N_i increases relatively steeply until the maximum, and then decreases gradually with increasing $\Delta\sigma$. Thus, both the shape and location of the peak of the $\Delta\sigma/\Delta\sigma_{design}$ versus n_i/N_i curve of the linear spectrum with n_{min} equal to 10^{-4} are the most analogous to those of the derived spectrum.

The fatigue life estimates based on the standardised linear and convex spectra with n_{min} equal to 10^{-2} and 10^{-4} at each detail of interest, as a percentage of the fatigue life estimates based on the derived spectra, are also given Table 5. For the three details of interest, the fatigue life values based on the standardised linear spectrum with n_{min} equal to 10^{-4} ranged between 18% and 23% of those of the derived spectrum.

Relationship between Fatigue Life and Design Loads

In an analysis of fatigue damage incurred in a United States Coast Guard Cutter, Stambaugh *et al.* (2014) concluded that it is important to monitor impact loading because the fatigue damage accumulated is proportional to the third power of the stress range. In line with this finding, the relationship between the design stress range $\Delta\sigma_{design}$ and the fatigue life at the three details of interest of the ACPB is quantified. For this exercise the fatigue life is estimated using the standardised linear spectra characterised by a 10^0 probability of the vessel sustaining between 30% and 100% of the design loads. The

subsequent fatigue life estimates for each percentage of $\Delta\sigma_{design}$, normalised by that based on the derived spectrum, are plotted in Fig. 11. Power functions are fitted to each detail's set of fatigue life values, and Eq. 5 is the average of the three functions. In Eq. 5 the power term of the inverse stress range is 3.9.
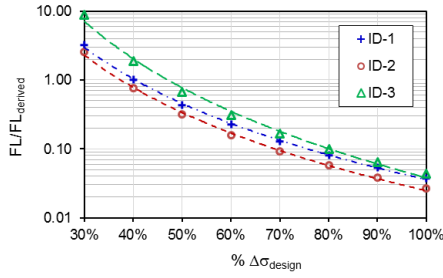

Fig. 12: Relationship between FL (fatigue life) based on standardised linear spectra and $\Delta\sigma_{design}$ at details ID-1, ID-2 and ID-3. Values of FL are normalised by that based on the derived spectrum, for each detail

$$\frac{FL}{FL_{derived}} = 0.033\left(\frac{1}{\Delta\sigma_{design}}\right)^{3.9} \qquad (5)$$

Discussion

Based on the above analysis, valuable further work includes establishment of the probability of exceedance of fatigue loads in the area of operations of the naval HSLC of concern. This would be similar to the approach employed in the Common Structural Rules (CSR) for Bulk Carriers and Oil Tankers (2010), in that dynamic sea pressures or fatigue loads are based on a 10^{-4} probability level of exceedance for the North Atlantic Wave Environment. However, naval HSLC operate in various wave environments and thus the probability of exceedance of fatigue loads vary. Also, in the CSR the characteristic load for fatigue assessment is an average value representing the expected load history reduced from the design load by a knock-down factor, rather than the maximum and minimum relevant seaway induced load effects. Given that the analysis presented is this paper indicates that the use of the stress range corresponding to design sagging and hogging load cases leads to conservative fatigue life estimates, even when a 10^{-4} probability of sustaining the design loads is considered, it is concluded that more characteristic fatigue loads for naval HSLC are required.

Eq. 5 illustrates that when the design loads are reduced by, for example, 10% the estimated fatigue life of the analysed details increase by approximately 50% assuming a linear stress spectrum. As the fatigue life is proportional to approximately the fourth power of the inverse stress range, it is important to predict and/or monitor the accumulation of fatigue damage over the lifetime of the vessel.

Clearly analysis of the fatigue life at the details of interest is heavily dependent on the representation of stress ranges, as well as other parameters. Thus, understanding of uncertainties in the analysis is critical. The uncertainties include:

- Applicability of rules-based design loads to deter-

mine the design stress ranges. The loads applied to the HSLC can feature a high degree of nonlinearity due to their hullform, operation in semi-planing or planing modes, and susceptibility to slamming (Magoga et al., 2014a).
- The dynamic behavior of the structure, that is, variation in the response frequencies and structural damping.
- Use of the structural stress approach in the fatigue evaluation at the details of interest, which is a compromise between accuracy and ease of use (Horn *et al.*, 2009).
- Assumption of linear scalability of the number of stress cycles incurred during the strain measurement period to the service life. This premise neglects the random nature of ocean waves over time. Strain monitoring during the entire life of the ship would be one way to mitigate this simplification.
- Uncertainty in the measurement of strains, due to uncertainty in the calibration of the strain gauges, induced electrical noise, and noise in the amplification system.
- Use of the Palmgren-Miner rule (Miner, 1945) which assumes that the effect of each cycle is independent and any resultant damage is linearly cumulative. Thus its weakness is that it does not account for load sequence effects.

The three details analysed are part of the ACPB engine room structure close to a pillar. As such, further investigation is required to extend the presented findings for reliable fatigue life evaluation at other structural areas.

Conclusion

Strain gauge data obtained from a hull monitoring system installed onboard a naval HSLC has been used to investigate stress spectra assumptions required in simplified fatigue analysis. Form fitting was performed to find the best model of the measured stress range data normalised by the design stress ranges. Then, using the structural stress approach, the fatigue life based on the derived and modelled stress spectra was calculated at three details of interest. It was found that, in comparison to the Linear and Weibull models, the fatigue life estimates based on Gaussian model correlated best to those of the derived spectra and fleet maintenance data. In addition, aggregate coefficients of the models are provided in order to inform the generation of stress spectra at structural details indicative of the joints of pillars and supporting structural items.

Driven by the experience of structural analysis of conventional ships, and the time-intensive and challenging nature of more sophisticated procedures, the applicability of standardised stress spectra in simplified fatigue analysis of naval HSLC was investigated. It was established that use of standardised linear and convex stress spectra characterised by a 10^0 probability of the vessel sustaining design loads during its lifetime leads to overly conservative fatigue life values. As such, strategies to better describe stress spectra include determination of

characteristic fatigue loads and probabilities in the area of operations.

Acknowledgements

References

(2006). "Welcome to the Armidale Class", Semaphore Issue 4. Sea Power Centre – Australia, Canberra, Australia.

(2010). "Common Structural Rules for Bulk Carriers and Oil Tankers". International Association of Classification Societies, London, United Kingdom.

(2013). "MAESTRO 11.0.0". DRS Defense Solutions, Stevensville, USA.

(2014). "MATLAB R2014a (8.3.0.532)". MathWorks, Natick, USA.

Aksu, S., Magoga, T. and Riding, B., (2015). "Analysis of HMAS GLENELG's Onboard Structural Monitoring Data", Pacific 2015 International Maritime Conference, Sydney, Australia.

Collette, M. and Incecik, A., (2006). "An approach for reliability-based fatigue design of welded joints on aluminunn high-speed vessels". Journal of Ship Research, Vol 50, No. 1, pp 85-98.

Det Norske Veritas, (2010). "Fatigue Assessment of Ship Structures, Classification Note No. 30.7", Høvik, Norway.

Det Norske Veritas, (2011). "Rules for Classification of High Speed, Light Craft and Naval Surface Craft", Høvik, Norway, Vol.

Engle, A., Lin, W., Salvesen, N. and Shin, Y., (1997). "Application of 3-D nonlinear wave-load and structural-response simulations in naval ship design". Naval Engineers Journal, Vol 109, No. 3, pp 253-265.

Fricke, W. and Paetzold, H., (2010). "Full-scale fatigue tests of ship structures to validate the S-N approaches for fatigue strength assessment". Marine Structures, Vol 23, No. 1, pp 115-130.

Fricke, W. and von Lilienfeld-Toal, A., (2008). "Annahmen von Beanspruchungskollektiven für Schiffskonstruktionen und deren Absicherung durch Messung". Materials Testing, Vol 50, No. 11-12, pp 721-728.

Gardiner, C., Vincent, P., Wilson, A., Ellery, D. and Armstrong, T., (2008). "A Trial Sensor Network for the Armidale Class Patrol Boat", Pacific 2008 International Maritime Conference, Sydney, Australia.

Germanischer Lloyd, (2013). "Rules for Classification and Construction Ship Technology, Seagoing Ships". Germanischer Lloyd, Hamburg, Germany.

Horn, A., Andersen, M., Biot, M., Bohlmann, B., Mahérault-Mougin, S., Kozak, J., Osawa, N., Jang, Y., Remes, H., Ringsberg, J. and van der Cammen, J., (2009). "TCIII.2: Fatigue and Fracture", Proceedings of the 17th International Ship and Offshore Structures Congress. Seoul National University, Seoul, South Korea, pp. 211-287.

Kramer, R., Rampolla, B. and Magnussen, A., (2000). "Fatigue of Aluminum Structural Weldments", SSC-410. Ship Structure Committee, Washington, United States.

Kramer, R.H., Haugan, G. and Fredriksen, A., (2006). "US navy high speed craft - Comparison of ABS and DNV structural requirements", Transactions - Society of Naval Architects and Marine Engineers, Vol 113, pp. 340-366.

Maddox, S.J., (2003). "Review of fatigue assessment procedures for welded aluminium structures". International Journal of Fatigue, Vol 25, No. 12, pp 1359-1378.

Magoga, T., Aksu, S., Cannon, S., Ojeda, R. and Thomas, G., (2014). "Identification of Slam Events Experienced by a High-Speed Craft", International Conference on Safety and Reliability of Ship, Offshore and Subsea Structures Glasgow, United Kingdom.

Magoga, T., Aksu, S., Cannon, S., Ojeda, R. and Thomas, G., (2015). "The Need for Fatigue Life Prediction Methods Tailored to High-Speed Craft: A Technical Review", Pacific 2015 International Maritime Conference, Sydney, Australia.

Mansour, A. and Liu, D., (2008). "Strength of Ships and Ocean Structures". The Society of Naval Architects and Marine Engineers, Jersey City, USA, Vol.

Matsuishi, M. and Endo, T., (1968). "Fatigue of metals subjected to varying stress", Japan Society of Mechanical Engineers, Fukuoka, Japan.

Miner, M., (1945). "Cumulative Fatigue in Damage", Journal of Applied Mechanics, Vol 12, pp. 159-164.

Phelps, B. and Morris, B., (2013). "Review of Hull Structural Monitoring Systems for Navy Ships", DSTO-TR-2818. Defence Science and Technology Organisation, Melbourne, Australia.

Sheinberg, R., Cleary, C., Stambaugh, K. and Storhaug, G., (2011). "Investigation of Wave Impact and Whipping Response on the Fatigue Life and Ultimate Strength of a Semi-Displacement Patrol Boat", 11th International Conference on Fast Sea Transportation FAST 2011, Honolulu, Hawaii, USA.

Soliman, M., Barone, G. and Frangopol, D.M., (2015). "Fatigue reliability and service life prediction of aluminum naval ship details based on monitoring data". Structural Health Monitoring, Vol 14, No. 1, pp 3-19.

Stambaugh, K., Drummen, I., Cleary, C., Sheinberg, R. and Kaminski, M., (2014). "Structural fatigue life assessment and sustainment implications for a new class of US coast guard cutters", Transactions - Society of Naval Architects and Marine Engineers, Vol 122, pp. 434-444.

Technical Committee CEN/TC 250, (1999). "Eurocode 9: Design of aluminium structures". British Standards, Brussels, Belgium.

Tuitman, J., Bosman, T. and Harmsen, E., (2013). "Local structural response to seakeeping and slamming loads", Marine Structures, Vol 33, pp. 214-237.